Research Square

Preprints are preliminary reports that have not undergone peer review.
They should not be considered conclusive, used to inform clinical practice,
or referenced by the media as validated information.

Development and testing of a low-cost RGB–depth camera and concept of operations for lunar south polar exploration in support of the Artemis program

C. Paige

c.paige@columbia.edu

Columbia, University

D. D. Haddad

Massachusetts Institute of Technology

A. Cook

FIG Technical Director

V. Jha

NASA Ames Research Center

A. N. Deutsch

NASA Ames Research Center

J. Shimada

NASA Ames Research Center

A. Colaprete

NASA Ames Research Center

F. Ward

R&D Engineer

A. Ekblaw

CEO and Co-Founder of Aurelia Institute, Central Square Cambridge

K. Pfrang

Senior Science and Technology Development Engineer

F. Meyen

Chief Strategy Officer

J. Heldmann

Principal Investigator, NASA Ames Research Center

D. Newman

Columbia, University

Article

Keywords: lunar exploration, Artemis, depth imaging, time-of-flight camera, ISRU, concept of operations, CLPS

Posted Date: November 27th, 2026

DOI: https://doi.org/10.21203/rs.3.rs-11782383/v1

License: This work is licensed under a Creative Commons Attribution 4.0 International License.
Read Full License

Additional Declarations: No competing interests reported.

Development and testing of a low-cost RGB–depth camera and concept of operations for lunar south polar exploration in support of the Artemis program

C. Paige[1]*, D. D. Haddad[2], A. Cook[3], V. Jha[4], A. N. Deutsch[5], J. Shimada[6], A. Colaprete[7], F. Ward[8], A. Ekblaw[9], K. Pfrang [10], F. Meyen[11], J. Heldmann[12], and D. Newman[13]

[1] Assistant Professor, Mechanical Engineering, Columbia, University, New York, NY, USA, 10027, 0000-0002-7857-8158. c.paige@columbia.edu
[2] Research Affiliate, Media Lab, Massachusetts Institute of Technology, 77 Massachusetts Avenue, Cambridge, MA, USA, 02139, 0000-0001-6420-3219
[3] FIG Technical Director, Flight Instrument Group, Bay Area Environmental Research Institute, Moffett Field, CA, USA, 94043
[4] Space Scientist and Flight Instrument Engineer, NASA Ames Research Center, Moffett Field, CA, USA, 94043, 0000-0001-9375-1505
[5] Planetary Scientist, Space Sciences & Astrobiology, NASA Ames Research Center, Moffett Field, CA, USA, 94043; Bay Area Environmental Research Institute, Moffett Field, CA, 94043, 0000-0001-9831-3619
[6] Systems Engineer II, NASA Ames Research Center, Moffett Field, CA, USA, 94043
[7] Director of the Science Directorate (Acting), NASA Ames Research Center, Moffett Field, CA, USA, 94043
[8] R&D Engineer, SpaceX, Los Angeles, CA, USA, 90250.
[9] CEO and Co-Founder of Aurelia Institute, Central Square Cambridge, MA, USA
[10] Senior Science and Technology Development Engineer, Lunar Outpost, Arvada, CO, USA, 80002, 0009-0003-7641-8948
[11] Chief Strategy Officer, Lunar Outpost, Arvada, CO, USA, 80002, 0000-0002-0140-6411
[12] Principal Investigator, Space Sciences & Astrobiology, NASA Ames Research Center, Moffett Field, CA, USA, 94043, 0000-0003-3397-1682
[13] Apollo Professor of Aeronautics and Astronautics and Director of the Media Lab, Massachusetts Institute of Technology, 77 Massachusetts Avenue, Cambridge, MA, USA, 02139, 0000-0001-6190-348X
** Corresponding Author*

Abstract
Acquiring high-spatial-resolution three-dimensional (3D) surface data at the lunar south pole is a critical enabler for in situ resource utilization (ISRU), geological field work, and immersive virtual reality mission operations support, capabilities identified as priorities by the Artemis III Science Definition Team Report. Here we report the development, ground-based testing, and spaceflight deployment of a commercial off-the-shelf (COTS) RGB-depth (RGBD) time-of-flight camera (the Microsoft Azure Kinect) aboard the Lunar Outpost MAPP rover on the Intuitive Machines IM-2 mission. The instrument was ruggedized for spaceflight to Technology Readiness Level 6, and a custom software application (AKALL) was developed to minimize power and data demands. Four testing campaigns validated a four-mode concept of operations covering dust interference, power and bandwidth constraints, field acquisition methodology, and optimal imaging parameters, with sub-centimeter reconstruction fidelity confirmed. Although the MAPP rover could not be deployed after the IM-2 lander tipped on landing, thermal telemetry confirmed camera survivability and a successful command uplink verified software integration. These results provide a validated, low-cost framework for RGBD depth-data collection on future CLPS missions in direct support of crewed Artemis surface operations.

Keywords: lunar exploration; Artemis; depth imaging; time-of-flight camera; ISRU; concept of operations; CLPS

Acronyms/Abbreviations

A3SDTR Artemis III Science Definition Team Report	ConOps Concept of Operations
AKALL Azure Kinect A La Lune	EVA extravehicular activity
CLPS Commercial Lunar Payload Services	ISRU In situ resource utilization
	MAPP Mobile Autonomous Prospecting Platform

MIT Massachusetts Institute of Technology
NASA National Aeronautics and Space Administration
PCB printed circuit board
POI point of interest
PSR Permanently shadowed region
RESOURCE Resource Exploration and Science of OUR Cosmic Environment
RGBD red green blue and depth
SEI Space Exploration Initiative
SSERVI Solar System Exploration Research Virtual Institute
ToF time of flight
TRL technology readiness level
VR Virtual reality

The future of human space exploration is undergoing a paradigm shift, anchored by NASA's Artemis program — the agency's primary strategic initiative to return astronauts to the Moon and ultimately send humans to Mars. With the advent of heavy-lift launch capabilities, an active Commercial Lunar Payload Services (CLPS) program, and a target first crewed lunar south polar landing in 2028 (Artemis IV), new enabling technologies are urgently needed to support safe, productive, and sustained human surface operations. One such required technology, as stated in the Artemis III Science Definition Team Report (A3SDTR)[1], is in situ instrumentation to support sampling and volatile monitoring that Artemis IV and V landings are targeting at the lunar south pole. This is a region where water ice in permanently shadowed regions (PSRs) is a target for understanding the origin and nature of volatiles in the inner solar system, and for evaluating the potential as an in situ resource utilization (ISRU) target and where Artemis IV will land the first humans since Apollo 17. The A3SDTR further specifies the need to convert raw surface data into processed, actionable information for tactical field decision-making[1], precisely the role that high-resolution three-dimensional (3D) mapping and virtual reality (VR) visualization can fulfil.

A VR platform can support lunar surface exploration by providing an immersive, three-dimensional (3D) construction of an exploration zone that can be used to provide situational awareness[2] and an in-situ scale reference system, train future astronauts[3] , enable scientific-based decision making[4,5] , increase accessibility and outreach opportunities[6] , and provide a basis for analysis tool development[1,7–11]. The efficacy of such a platform scales with the resolution of data used in reconstruction, and most existing lunar surface datasets fall far short of the sub-meter spatial resolution required to support the extravehicular activity (EVA) planning, geological field work, and ISRU site characterization that Artemis astronauts will need at the south pole. For example, topographic polar data acquired by the Lunar Orbiter Laser Altimeter (LOLA) used to model the 3D landscape has a radial elevation accuracy of 10 m[5].

Existing VR platforms have been used successfully in planetary science applications, typically relying on scene reconstruction using structure from motion (SfM) photogrammetry[5]. The SfM photogrammetry, however, is limited by a reliance on large datasets (and thus large data volumes and transmission bandwidth needs) with significant image overlap and similar optical parameters, plus an arduous alignment process, often requiring iterative human supervision, to reconstruct 3D point clouds. Furthermore, SfM photogrammetry relies on an external light source to illuminate the imaged area, limiting its use for reconstructing permanently shadowed regions (PSRs) and enclosed lava tubes, which are major areas of scientific exploration interest for the Moon[1,10–12] .

There are three major classes of depth cameras: (1) structured or coded light, (2) stereo depth, and (3) time-of-flight (ToF) or LiDAR. The first uses the deformation of a known light pattern to calculate distance to an object, which, like SfM photogrammetry, is challenging in poorly illuminated regions. The second uses the known distance between two cameras and the light reflected off an object for triangulation. The third calculates distance using the timed return of laser light reflected off a surface; the stronger the laser used, the greater the distances ToF cameras can measure. Both structured light and ToF cameras require that the returned light be clearly distinguishable as the reflected emitted light, and so can be susceptible to interference from external light sources (including sunlight). This interference is not of concern when exploring sub-surface structures (e.g., lava tubes), PSRs, or during the lunar night. An additional benefit of ToF cameras is their increasing use in commercial industry; commercial-off-the-shelf (COTS) components are now readily available and can be made flight ready, as we demonstrate here for lunar operations. To overcome these limitations, we propose using a ToF depth camera for high-spatial-resolution 3D scene reconstructions, an approach well suited to the PSR exploration, EVA site survey, and ISRU prospecting priorities of

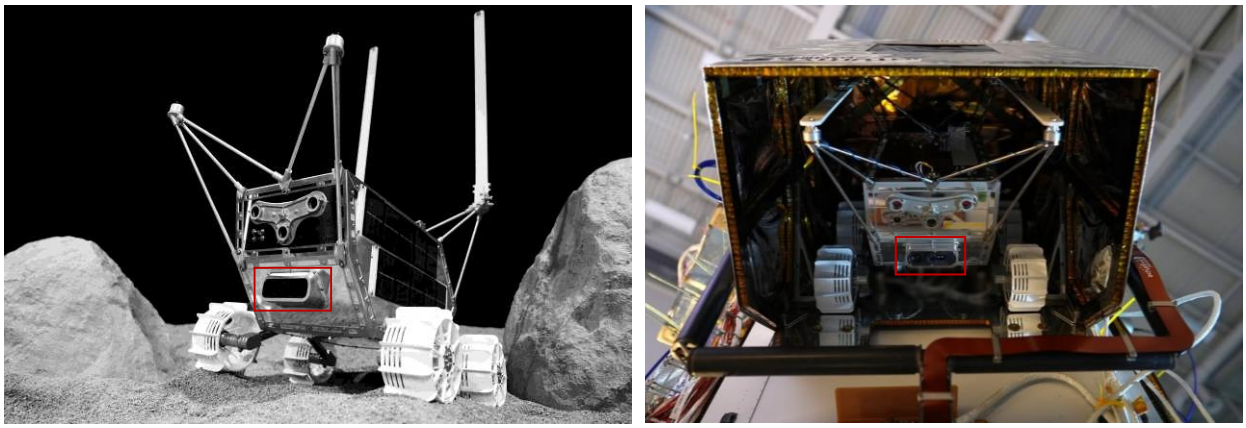


Fig. 1 | Lunar Outpost MAPP rover model. Left – display model of the Lunar Outpost MAPP rover with integrated Microsoft Azure Kinect (outlined in red) and right - 3D model of the Lunar Outpost MAPP rover with the modified Microsoft Azure Kinect camera (outlined in red) integrated on the front face of the rover.

the Artemis program[1,11] .

As part of NASA's Solar System Exploration Research Virtual Institute (SSERVI) Resource Exploration and Science of OUR Cosmic Environment (RESOURCE) project, and in collaboration with NASA Ames Research Center and Lunar Outpost, we prepared the Microsoft Azure Kinect, a COTS RGB + ToF camera (RGBD camera)[13], for lunar exploration and developed integration pathways for translating depth mapping into an accessible VR platform. The VR platform focuses on cm-scale resolution imagery (ex: 1-5 cm rocks, and micro PSRs, < 10 cm) and depth-data for geological and scientific analysis of the lunar surface. Based on field test performance evaluations, a RGBD camera was selected to provide the most comprehensive mapping while minimizing data-return bandwidth and development costs[7,14]. The RESOURCE team developed the hardware, software, and concept of operations (ConOps) for the modified Kinect. The Kinect was integrated into the LV1 MAPP rover, a sub 20-kg exploration-class rover from Lunar Outpost and manifested on the Intuitive Machines (IM) Nova-C lander, which was intended to land and operate in the lunar south polar region for 9 Earth days (one lunar daylight cycle)[13], as part of the Intuitive Machines mission (IM-2), Fig. 1. Although the MAPP rover was unable to be deployed due to the IM lander tipping into a crater, this was the first ToF camera on the lunar surface. With real-time downlinking of data, images of craters and boulders gathered by the Kinect on the lunar surface were planned for navigation use alongside on-board rover sensors. With possibilities of manifesting the camera on future lunar south polar region missions, once successfully deployed this camera will test the capabilities of this technology in the lunar south polar region, providing a framework for future low-cost depth-data collection payloads. The CLPS program was established specifically to serve as the robotic reconnaissance arm of the Artemis program, scouting resources, testing ISRU technologies, and acquiring surface data in the lunar south polar region ahead of crewed Artemis landings; this mission represents a direct contribution to that preparatory effort.

The RESOURCE hardware will serve as a technology demonstration for surface depth-data acquisition and will provide high spatial resolution data for in situ resource utilization (ISRU) analysis. With this project, our specific objectives were to:

1. Modify and test a COTS RGBD camera for use in a spaceflight environment.
2. Increase the spatial resolution of surficial RGBD data at the IM-2 lunar exploration region.
3. Develop the processing pipeline for rendering immersive 3D environments in VR from collected data, to support Artemis astronaut EVA planning, real-time situational awareness, and post-traverse geological analysis.
4. Develop a flexible concept of operations (ConOps) for depth-data acquisition.
5. Map and characterize micro cold traps and small-scale (cm to m) lunar topography and texture.

Here we discuss the testing and development work completed to prepare the hardware, software, and ConOps for the MAPP rover. We deduce data requirements, including rover motions needed to achieve optimal VR reconstruction quality. We also discuss the development of the ConOps for the 9-Earth-day mission with major considerations for power and data bandwidth limitations, as well as optimization of the VR rendering pipeline.

2 Results

2.1 Space Flight Qualification of the Microsoft Azure Kinect

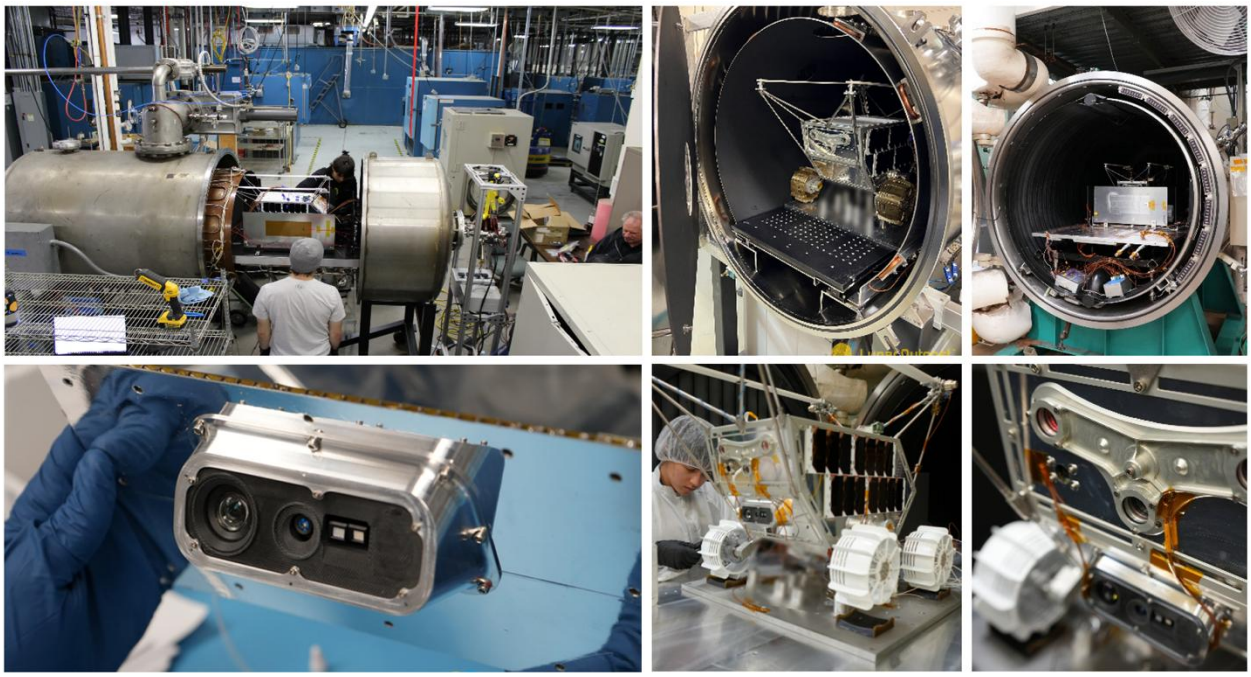


Fig. 2 | Microsoft Azure Kinect integrated on the Lunar Outpost LV1 MAPP rover undergoing testing with the Engineering Model and Flight Model MAPP vehicles. Top row: thermal balance (left), qualification (middle) and acceptance testing (right), bottom row: Kinect camera integrated onto front panel (left), before undergoing thermal vacuum acceptance testing (middle) and temperature sensor placement (right).

The Kinect was evaluated for flight-compliant materials and modified to reduce mass by the Flight Instrument Group at NASA Ames[13]. Mass was reduced by 140 g after removing the outer aluminum casing, the microphone array, RF shield and front face. Plastic parts were replaced with vacuum-compatible materials and cables were replaced with specialized cables for integration into the Lunar Outpost MAPP rover. The environmental testing was performed on the modified Kinect with random vibration/sine testing, per NASA's General Environmental Verification Standard (GEVS) for spaceflight launch survival. Thermal vacuum testing cycled the instrument between expected hot (+80ºC) and cold (-3 ºC) survival temperatures, as well as +50ºC and 0ºC operational temperatures. The instrument functioned nominally at the conclusion of vibration and thermal cycling tests and the camera was flight qualified to TRL 6[13]. When installed on the Lunar Outpost MAPP rover, operational temperatures were maintained by a camera heater, and temperatures were monitored by two sensors, one thermocouple applied to the top flexible surface connecting the RESOURCE Camera PCB to the MAPP body, the second applied directly to the inward facing side of the PCB.

In addition to vibration and vacuum qualification testing, shown in Fig. 2, the Kinect camera, integrated onto the MAPP rover, underwent a series of drive testing and Mission Operations scenarios to better understand the instrument operations and prepare the science teams. shows the Engineering Model of the MAPP rover with the Kinect camera



Fig. 3 | Field testing of the Lunar Outpost LV1 MAPP rover Engineering Development Unit. Drive testing at Lunar Outpost's Southern Colorado Autonomous Test Facility (left) and mission operations testing in Lunar Outpost simulant testbed (right)

installed as it drives at Lunar Outpost's outdoor Autonomous Testing Facility, simulating craters, berms, and other obstacles, Fig. 3. The vehicle and integrated payloads conducted training activities at Lunar Outpost's simulant testbed where lighting and obstacles were simulated for accurate data and image captures.

2.2 Software Development

To integrate with the Lunar Outpost rover operating system, we needed to develop a custom software application. Additionally, we needed to be able to parse single frames from the standard Kinect video capture mode to minimize bandwidth for downlinking data. The software development is described in detail in Haddad et al., 2024[15] and summarized here. We used the Microsoft Azure Kinect C and C++ to design the Azure Kinect à La Lune (AKALL) software to control the camera and capture data from the RGB camera, the ToF camera, and the IR sensor. The application was designed within a Docker container running Ubuntu 18.04 LTS, providing an isolated and portable environment for it to operate in. The application communicates with the rover UNIX socket protocol by implementing a UNIX socket server using Python3. The socket server enables the application to control the camera using custom capture sequence inputs that we have implemented. For example, for the command sequence K15MJPG07201 breaks down to K for Kinect camera, 15 for the frames per second (fps), MJPG for the compression used for the RGB image, 0720 represents the resolution of the RGB image and 1 is the depth-mode used. Table 1 shows the full list of options for the command sequences. While all the options have been made available for the flight software, ConOps testing provided the optimized settings for each of the capture modes.

Table 1 | Command code sequence breakdown for the AKALL software. Top shows an example code with breakdown of meaning, bottom shows all options for each command code component.

Camera Setting	Available Options
Frames per second (FPS)	5, 15, 30
Compression format	MJPG, NV12, YUY2, BGRA, DP16, IR16
Resolution	720, 1080, 1440, 1536, 2160, 3072
Depth mode	Narrow field of view, unbinned (75x65)
	Narrow field of view, 2x2 pixel binning (75x65)
	Wide field of view, unbinned (120x120)
	Wide field of view, 2x2 pixel binning (120x120)

The camera allows for additional specifications for the RGB camera settings, which have been included in the control sequences as optional components. These include the ability to specify exposure, contrast, sharpness, gain, white balance, black light compensation, power line frequency and timestamp. As with the depth camera settings, AKALL includes all these settings as options but will only use the optimized selections for the specified capture modes.

2.3 Concept of Operations Development

The Microsoft Azure Kinect camera can operate in one of four modes: 1) Near Field-Of-View (NFOV), 2x2 binned (2x2 square of pixels is binned into a single pixel) 2) Wide Field-Of-View (WFOV), 2x2 binned, 3) NFOV, unbinned, and 4) WFOV, unbinned. These modes determine the field of view of the camera (narrow or wide) and light sensitivity (binned or unbinned). These methods have implications for both the instrument data budget as well as quality for output imagery. Our primary concerns for this mission are power consumption and data minimization, as both are heavily restricted. Our ConOps attempt to optimize both for different image resolutions. Four capture modes are planned for this mission: 1) Single Target capture, 2) Traverse capture, 3) Science Station capture, and 4) Single Target Circumference capture. These are described below. Nominally, the Microsoft Azure Kinect takes video recordings which are processed as point-clouds. To minimize data requirements, we save only a single frame from within the video recordings containing the RGBD channels using AKALL, which can later be stitched together for a composite point-cloud. Although this may reduce the accuracy of the image, the data reduction is crucial for mission operations.

2.3.1 Single Target Capture

This mode captures single frame RGBD images of points of interest for which there is minimal time or data availability for capture from multiple view angles. The data can be used to recreate a directional 3D image of the

feature. Because this is a single capture, occlusion of data would limit the functionality of this mode and should not be used where complete scene reconstruction is required or available.

2.3.2 Traverse Capture

This mode captures single frame RGBD images on the rover's traverse path. Ideally this would be done every 1 m allowing for overlap between image captures, for ~10 m sections of traverse. Here the traverse path is expected to be relatively straight, however, given each capture can view up to 3 m at high resolution, the image per 1 m capture frequency allows for sufficient overlap for a relatively widely varying traverse path as well. This data will be used to create a 3D traverse path model (corridor of DEM data). As with the single target capture mode, occlusion would provide only a partial 3D reconstruction, missing data from the backs of target objects.

2.3.3 Science Station Capture

This mode captures a complete site by performing a raster pattern approach over the selected location and capturing single frame RGBD images at 1 m intervals over the entire site. This method provides the same 3D corridors described in the Traverse mode, however, using the raster pattern, provides the reverse direction as well with sufficient overlap between corridors to construct a complete 3D scene. This data can be used to create a 3D science station environment at locations of interest (ex: impact ejecta site, approach to challenging terrain, sites identified as high probability of water content, etc.).

2.3.4 Single Target Circumference Capture

This mode aims to capture all angles around a single target object. These captures should be taken every 30º relative to the object's center, or for very large objects, as many as necessary to have ~20 º of overlap at each edge between frames. This data will be used to create a full 3D reconstruction of all visible areas of the object, including lighting conditions, color, and geometry. This capture type places the most significant demands on rover operation and is variable depending on mission constraints. The current mission has the camera on a stationary mount and thus requires the rover to translate and rotate around the object with relatively good precision. The high degree of overlap between images helps to reduce this challenge, however future missions would benefit from gimballing and a rotatable camera platform. For any capture, the target distance must be no greater than 4 m from the surface of the feature, and no less than 0.5 m for best resolution data, ideal distance is 1 m.

2.4 Power and Data Rates

The baseline power requirements taken as part of the initial hardware assessment are shown in Table 2. The camera draws no power when off and remains at a minimal 0.57 W when idle. The camera's power draw increases to a maximum of 1.08 W (settings to WFOV, binned, BGRA compression, 2160p RGB resolution and 30 fps). This is within Lunar Outpost's maximum allowable power draw and should be considered the worst-case-scenario as the AKALL software does not require the power used for the SDK graphical displays when operating the video streaming application.

The results from the power and data requirements experiments are shown in Table 2 (baseline power draw) and Table 3 (optimized capture mode settings). The calculations for total data required for each capture mode are made based on the optimized camera settings. For a single image capture, to ensure the depth image is completely within the color image (full overlap), we maximize depth resolution while minimizing color resolution at the 4:3 ratio. We use the unbinned, NFOV (640x576) depth image resolution, with 1536 (2048x1536 - 4:3) color resolution. The data requirement is 728 KB for the color image and 737 KB for the depth image, thus 1.465 MB per image. The power required for the single image capture is 1.02 W. For the traverse capture mode, we again use complete overlap of color and depth images (4:3 ratio for color image), but now minimize both color and depth resolution to maximize the number of images we can take. This results in a NFOV, 2x2 binned (512x512) depth image resolution, with a 1536 (2048x1536 - 4:3) color image resolution. The data requirement is 184 KB for the color image and 737 KB for the depth image, thus 0.921 MB per image. The images are taken every 1 m, thus the data requirement is scaled by the length of the traverse. The power required for the traverse capture mode is 1.08 W. The Science Station capture mode uses the same optimized parameters as the traverse capture mode and thus scales with the number of images required. For example, a 5 m x 5 m site would require 6 x 6 image captures taken in a raster-like pattern. This would require 33 MB, within the Lunar Outpost data download limits. Finally, the circumferential capture mode follows the same optimized camera settings used for the single capture mode. For a small feature or rock (<1m) this would require 12 images, totaling 17.58 MB.

Table 2 | Baseline Power Draw requirements for various settings on the Microsoft Azure Kinect.

Mode	Maximum Power Draw (W)	Settings at Max. Power Draw
Off	0	NA
Idle (no programs open)	0.577	NA
Idle (viewer open, not streaming)	0.566	NA
Streaming in viewer	1.082	WFOV, Binned, BGRA, 2160p, 30 FPS
Recording (Viewer Closed)	1.077	NFOV, Unbinned, 2160p, 30 FPS

Table 3 | Optimized capture mode settings.

Scenario	Number of images	Data requirement	Power requirement per image	Optimal camera settings
1 - Single	1	2.20 MB	1.02 W	K30MJPG15362
2 - Traverse	1/meter	0.92 MB per meter (ex: x 10m = 9.2 MB)	1.08 W	K30MJPG15361
3 - Science station	1/meter	0.92 MB per meter (ex: 5m x 5m site -> 6x6 images -> x 36 = 33 MB)	1.08 W	K30MJPG15361
4 - Circumferential (25 cm object)	12	2.20 MB per image (ex: x 12 = 17.58 MB)	1.02 W	K30MJPG15364

2.5 Software Concept of Operations Results: NASA SSERVI Lunar Testbed

The NASA SSERVI lunar regolith testbed at NASA Ames Research Center is a 4 m x 4 m x 0.5 m testbed containing 8 tons of JSC-1A lunar lowland simulant. The testbed was used for a 2-day test campaign to assess optimal lighting conditions, resolution capabilities in a lunar simulated environment, and data capture mode operations. During the test campaign, the testbed contained a simulated crater as well as small rocks (1-10 cm) and mass wasting features (rockslides and debris flows) that were imaged to test the single capture mode, the circumferential capture mode, and a future mode in which a gimbal may be available (enabling changes in camera angle). The capture modes were tested using the AKALL software and compared against a modified version of the Open3D library and software[16–18]. We used Open3D to capture, process and visualize the data recorded by the RGBD camera, enabling us to generate 3D models with a high degree of accuracy and detail from single recordings. Three-dimensional reconstructions of the environment allowed us to analyze the highest obtainable resolution of features and the optimal rover position with respect to sun angle to minimize washout.

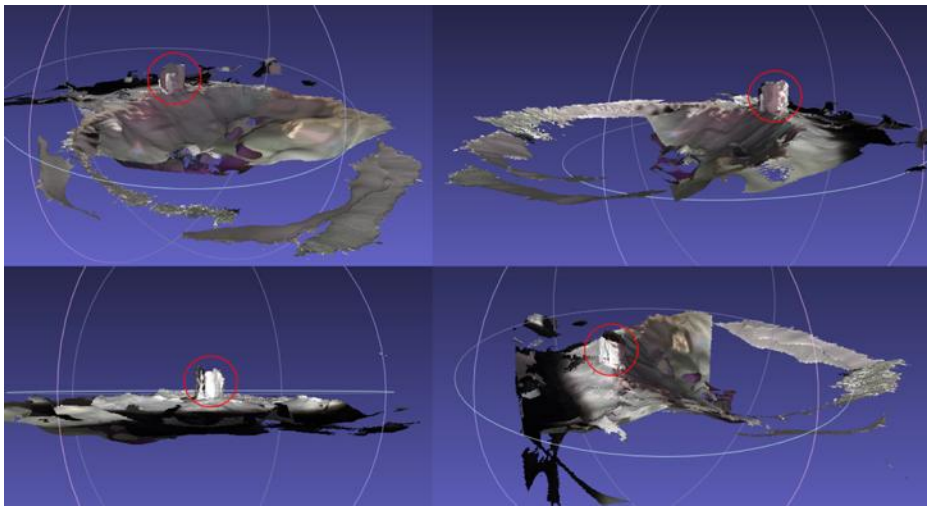


Fig. 4 | 3D reconstruction of large rock using 6 individual 3D images manually stitched in MeshLab. Red circle shows large rock, 24 cm high by 12 cm wide by 14 cm deep .

The AKALL software functioned as expected when collecting the data at the NASA SSERVI lunar testbed. Data requirements were confirmed and download formatting was effectively demonstrated. Because the AKALL software requires custom rendering capabilities, which had not yet been developed, we used the Open3D software to capture motionless videos (camera was held steady during recording with no motion in the scene) that were representative of the single image captures taken by the AKALL software. Open3D was then used to render these stills into 3D images representative of what was observed with the AKALL captures. These were then stitched together using MeshLab to create 3D scenes. We then assessed the stitched single ima ge capture methodology versus continuous video capture with movement. This also provided the data pipeline to be used once the custom rendering software is in place. The experiment conducted at NASA Ames also provided insights into the degrees of overlap required for a complete circumferential 3D reconstruction, optimal sun direction, and obtainable feature resolution. Here, we examine the results from the circumferential capture mode for a large rock test for degrees of overlap, the single image capture mode, while changing the direction of the light source around a crater to test the optimal sun direction and for a comparison of image reconstruction versus reconstruction from video, and a single image capture mode test of a boot print and the crater both for obtainable feature resolution.

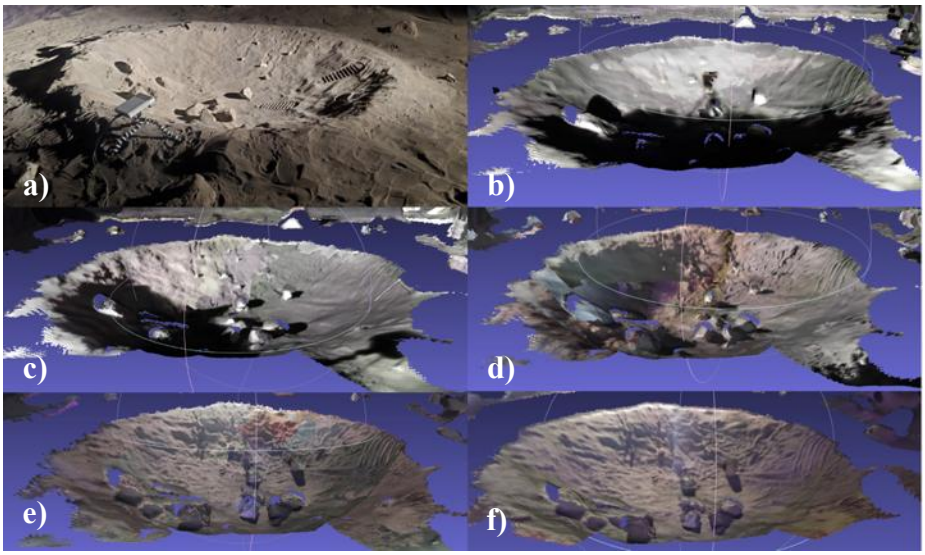


Fig. 5 | 3D reconstructions from SSERVI Lunar Regolith Lab. a) Photo taken of crater experimental setup (ground-truth), b)-e) 3D reconstruction (5 images: yaw left and right, pitch up and down and neutral). b) 0º, c) 60º, d) 120º, e) 180º. f) 3D reconstruction from continuous video capture of yaw left, right, pitch up and down.

Fig. 6 shows views from four different angles of the large rock reconstruction. This was a compilation of 6 images, taken at 60º intervals with the lighting held constant for all 6 image captures. While we were able to reconstruct the rock, it had to be done by manually co-locating points from each 3D image. To use an automated stitching function, a larger degree of overlap would be necessary. Additionally, the image resolution was below the cm-scale requirement because of the inability to stitch the images more accurately. For

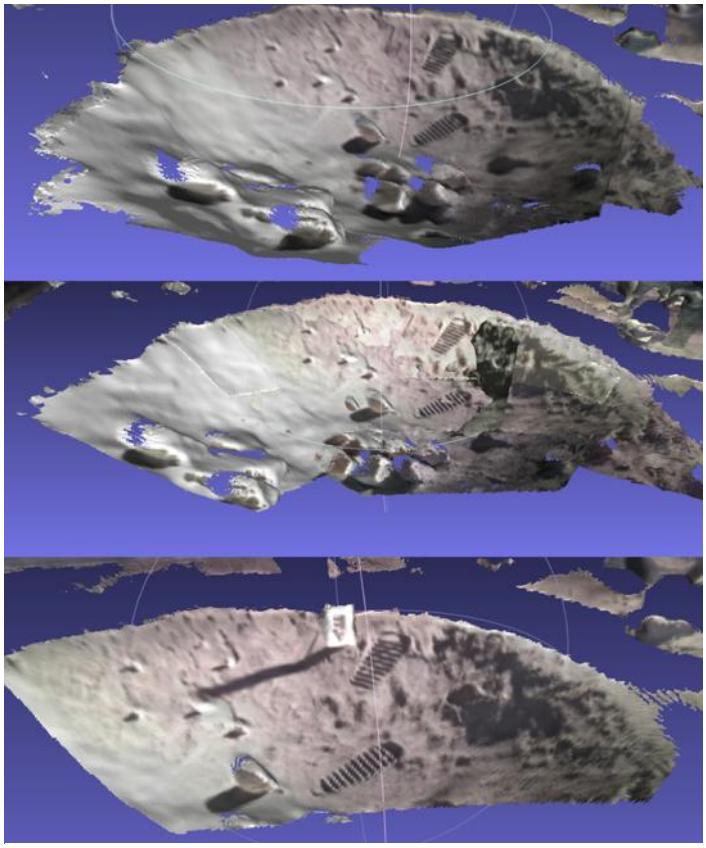


Fig. 6 | 3D reconstruction of a boot print. Top - from continuous video, middle - from 5 image captures and bottom - single frame reconstruction, image includes scale card with 10 cm downward facing arrow. Boot print is 25 cm long by 12 cm wide with treads 1.5 cm wide and 0.5 cm deep.

this reason, the ConOps was modified to take images every 30º instead of every 60º. While this does double the data requirement for the circumferential capture mode, it is still within the data limits and will dramatically improve the accuracy of the stitching and the resolution of the image.

Fig. 5 shows the crater, reconstructed using the 5 individual camera positions (yawed, pitched and neutral) for the 0º (B), 60º (C), 120º (D) and 180º (E) sun angle positions. Here we see that at 0º much of the resolution is lost in the reconstruction due to the sun angle. The optimal sun angle appears to be at 120º (or equivalently 240º), although the 180º sun angle surprisingly has similar resolution to the optimum angle. We also show the 3D reconstruction of the same movements (yaw and pitch) in a single continuous video with the sun at 180º (F). Comparing the stitched image captures to the continuous video we see that very little, if any, resolution is lost. This suggests the image stitching methodology adopted for this ConOps to reduce the data requirement will not reduce the resolution of the 3D reconstruction.

Fig. 6 shows a reconstruction of a 3D printed print from the 5 camera orientations (yawed, pitched and neutral) as well as the 3D reconstruction from the continuous video of the movements. We also include a 3D image with a scale card. Here, we see minimal resolution loss for the stitched reconstruction compared to the video reconstruction, the same as for the crater, although there is some distortion from color variation due to the change in camera position in the stitched reconstruction. This may be improved by further processing of the images. The scale card shows an arrow with a single vertical bar extending up and two horizontal bars extending out from the vertical bar. The arrow and vertical bar are each 5 cm long and each horizontal bar is 1 cm wide. Using this scale bar as well as the known slat sizes in the boot (25 cm long, 11 cm wide with treads 1.5 cm apart and 0.5 cm deep) we can see that we can achieve accurate sub-cm resolution with either the single image capture or the multi-image reconstruction for both the RGB and depth cameras.

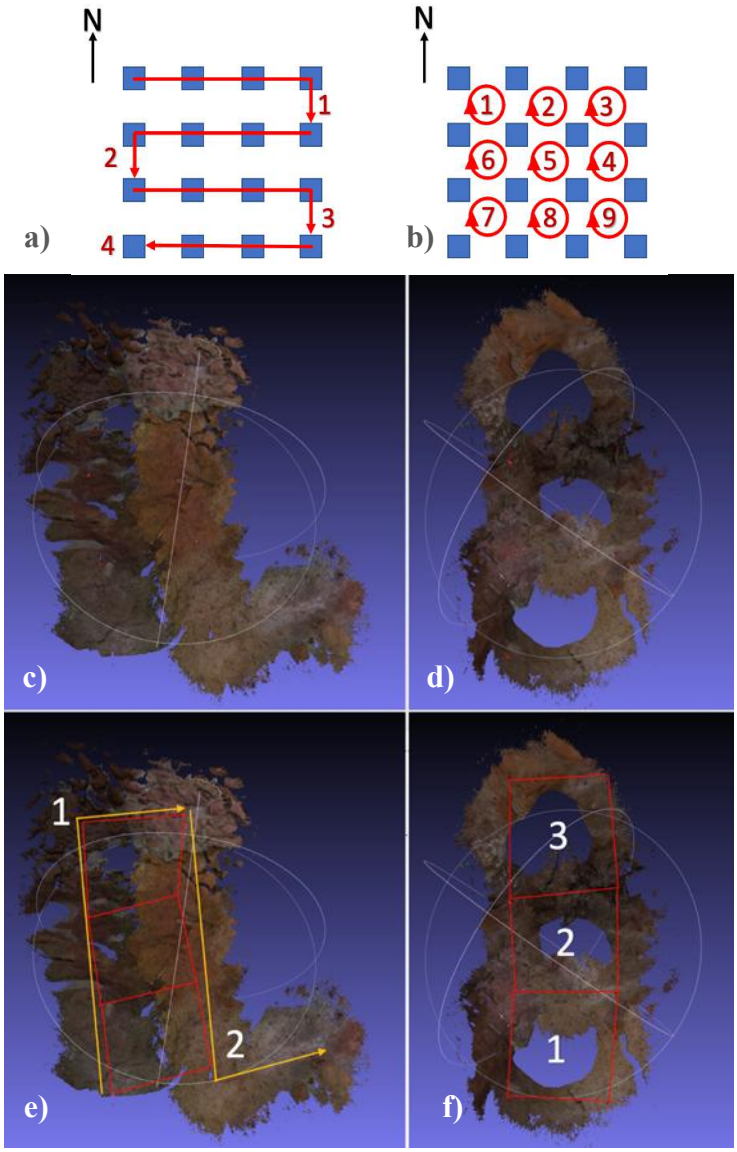


Fig. 7 | Microsoft Azure Kinect recording patterns in Svalbard, Norway. a) Raster pattern (better for post-processing) – 4 recordings and b) Grid pattern – 9 recordings 3D reconstruction for Svalbard, Norway capture. c), e) images were captured using raster pattern (traverses 1 and 2 shown on e)), d), f) images were captured using grid pattern (captures 1, 2 and 3 on f)). Red squares indicate 3.3m x 3.3m marked grid blocks.

2.6 Concept of Operations in Svalbard, Norway

The Microsoft Azure Kinect was field-tested in Svalbard, Norway to assess two different capture styles, a repeated grid-style data capture, as well as a raster-style data capture (Fig. 7A)[19]. Svalbard is an archipelago in the Arctic circle between Greenland and Norway. The exposed geology, minimal vegetation, and tundra conditions (low temperature

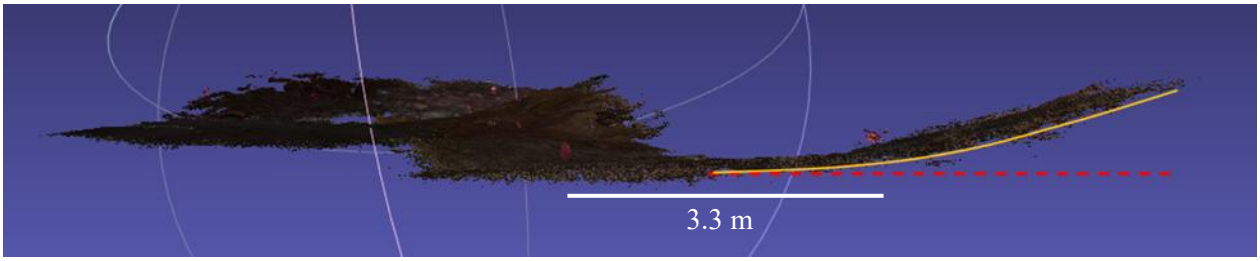


Fig. 8 | Side view of 3D reconstruction of combined raster pattern. Red dashed line indicates where the ground should be, orange solid line indicates where the ground is in the 3D reconstruction due to IMU drift.

and humidity) make it a valuable planetary surface analog. Using Svalbard, Norway as a planetary analog, we tested preliminary ConOps for data collection techniques with the Microsoft Azure Kinect in concert with the development of a virtual environment to test the effectiveness of VR for lunar and planetary surface exploration, field methodology was reported in Paige et al., 2023[19] and Paige et al., 2024[8].

The data collected on the RGBD camera was captured as a .mkv video file containing both depth and RGB data on Open3D[16,18]. Using Open3D, we generated a 3D image (.ply file) for each recording. We then attempted to stitch together the 3D reconstructions for a complete science station (10 m x 10 m field site) using MeshLab[20].

Stitching together raster 1 and raster two (Fig. 7, C and E)), we completed a 3D reconstruction of the first three grid blocks. We then stitched together grids 1, 2 and 3 from the grid method (D and F). These 3-grid corridors from each collection method are shown in Fig. 7. It is clear from this comparison that the grid method has large blank spaces left from where the camera was held. If this method were to be used, the grid block's size would need to be reduced by at least half to ensure complete coverage of data between the two captures. The raster pattern provided a more complete coverage of the 3 grid blocks as well as providing data outside of the 10 m x 10 m field site. Additionally, these were captured using continuous video stream. When using the single image capture operation planned for the Lunar Outpost mission each grid block would require 12 images to complete the capture for a 1 m block (allowing for increased overlap), while the raster would only require 12 per 3 m grid block (3 along each border) as there is already sufficient overlap that the interior of the grid would be captured from a 3m x 3m grid block. From this experiment, we found that the traverse mode and the science station mode were best captured using the raster-style collection method.

While the raster method did provide a lower data requirement for a 3D reconstruction with more coverage, we did find an inherent complication in this collection method. The IMU appeared to experience drift over the course of a traverse, resulting in a curved surface in raster 2 which should have been flat, Fig. 8. This made it impossible to complete the full 10m x 10m site reconstruction. We expect that this problem will be alleviated in the mission ConOps as we will be taking single image captures as opposed to continuous video, but the issue should be noted for future missions where video may become an option. Additionally, we will be using the Lunar Outpost rover's IMU for position information, which again, should ensure this is not a problem on the mission.

2.7 Dust Interference in Lunar Gravity

Lunar dust is one of the primary challenges of returning to the lunar surface. It is 'very abrasive, highly cohesive, [and impairs] optical instrumentation'[21]. To prepare for flight-readiness testing of the COTS part, in addition to vacuum, temperature and vibration testing, we needed to determine the capabilities of the camera for two lunar dust considerations: 1) the ToF camera data collection capabilities with dust interference, or veiling [21] and 2) visibility with lens occlusion from dust exposure. The test was performed during two parabolic flights. Primary tests were completed in 2022 with mission-representative tests conducted in 2024. Both experimental setups emulated the MAPP rover configuration, with the Kinect positioned next to a rover wheel in a containment box with lunar regolith simulant. The Kinect's data capture capabilities were assessed using a 3D printed rock wall opposite the camera with an LED illuminating the scene.



Fig. 9 | Small amounts of dust on the Azure Kinect camera after the 2022 parabolic flight. Dust is visible as light gray accumulation on the lens (left), cords and body (right).

Dust accumulation was observed on the Azure Kinect camera lens, Fig. 9. Although the dust on the lens was not the largest

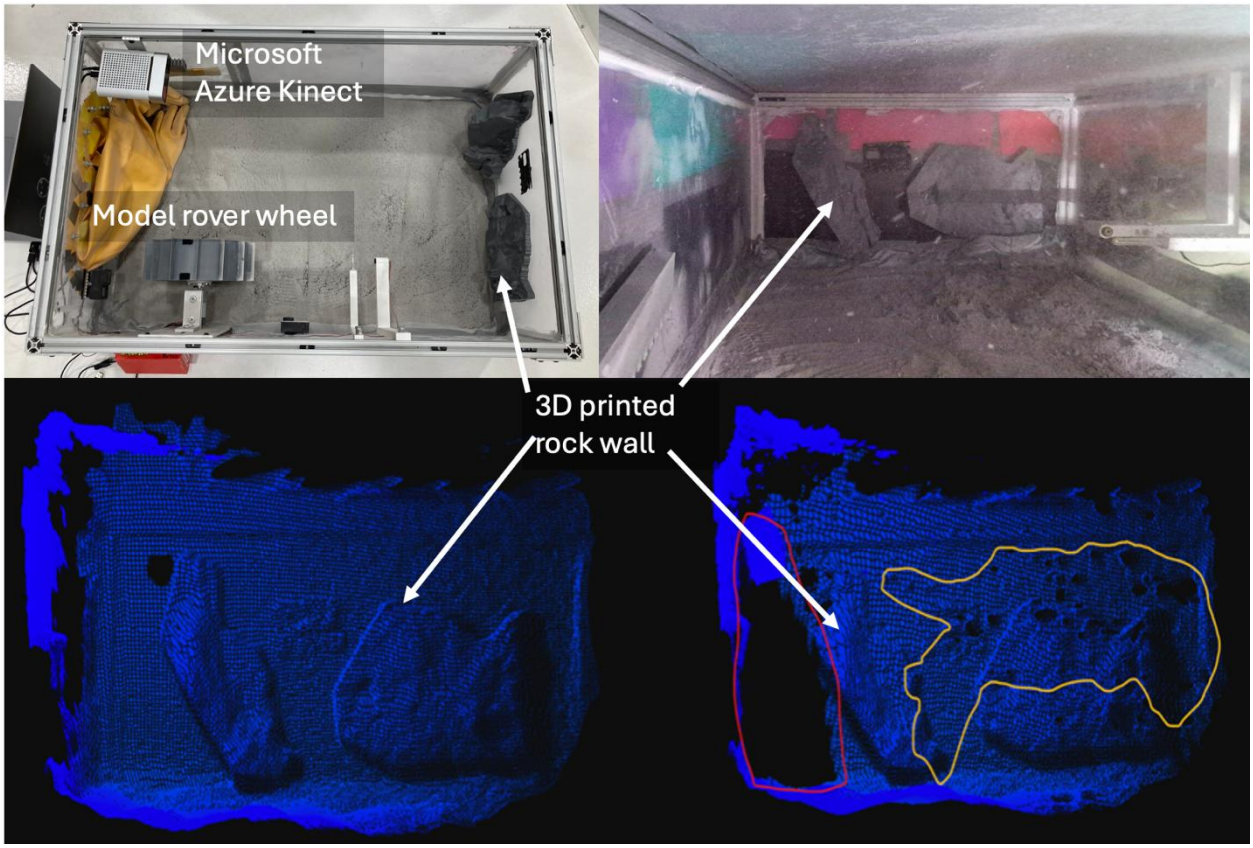


Fig. 10 | RGBD data captured with the Microsoft Azure Kinect during 2024 parabolic flight. Experimental setup (top left), interior view from RGB camera of experimental setup showing 3D printed rock wall (top right), Parabola 2 in Lunar gravity (bottom left), Parabola 7 in microgravity (bottom right) - yellow zone shows area where dust kick-up interference is visible, red zone shows where a loose tool caused a blackout zone.

contributor to the interference it clearly was beginning to create a dust film on the lens. Over time this would increase and would eventually become the greater issue for camera recording.

Data collected on the 2022 was only in microgravity and reported in Moreno et al., 2022[22]. This data provided baseline confirmation of the camera configuration, minimal dust adhesion for worst-case scenarios, and resolution limitations for worst-case scenarios.

During the 2024 flight, the wheel was successfully operated and RGBD data was captured for 10 parabolas. Given the 2024 test configuration more accurately matched the flight configuration, this data was considered to ensure flight readiness. During the Martian and lunar parabolas (1-4), no dust kick-up was recorded by the RGBD camera, and the image resolution was maintained. During parabolas 7 and 8 (microgravity), dust particles were observed in the video and did cause interference with the rock wall. Parabolas 2 (lunar gravity) and 7 (microgravity) are shown in Fig. 10 for comparison with the images taken 10 s into the altered gravity. Given parabolas 5-10 were in microgravity, this does not pose a concern for the mission but does indicate that ideally the camera should be positioned on the front of the rover to avoid this possible interference in a rear-facing configuration.

Interestingly, the data collected during the microgravity parabolas showed similar behavior to what we would expect in lunar gravity. Because the gravity during a parabola is not exact and the lunar simulant is fine-grained, we can observe these fluctuations in gravity. For instance, the larger dust formations clearly fall back to the base of the box during the parabola as opposed to continuing in their trajectory as we would expect for microgravity. Because of this we can interpret the data to provide at least an insight into the dust interference patterns for lunar gravity as well.

2.8 Mission Operations Preparation

In advance of the IM-2 mission, the MIT and Lunar Outpost Mission Operations teams conducted multiple operations scenarios including drive testing with the vehicle and integrated instruments to train expected operations and understand vehicle behaviours, including expected data. Further operations testing subjected Mission Operations teams to expected and contingency scenarios including rover egress from the lander, image and data captures, and

charging operations to prepare both vehicle and instrument operators for the harsh and often unexpected lunar environment. Mission Operations training was conducted with both the MAPP Engineering Model in-the-loop as well as the Lunar Outpost Stargrid Digital Twin with instrument, avionics, drive characteristics, and power models integrated. All testing was completed with Lunar Outpost's Stargate, ground station and telemetry management software, to best prepare mission operators as they would operate the vehicle and instruments in space.

2.9 Intuitive Machines 2 Mission Results

MAPP launched from Kennedy Space Center (KSC) onboard a SpaceX Falcon 9 rocket, as a part of the IM-2 lunar lander mission on 26 February, 17:17 MT, Fig. 11. MAPP rover turn-on was accomplished post Launch Vehicle Separation on 26 February, 18:52 MT and initiated collecting of data by the rover and sending it to the lander, where it was stored for downlinking to Earth during Store and Forward windows provided by IM. Transit occurred after Launch Vehicle Separation and included the voyage from Earth orbit to lunar orbit. During transit the MAPP rover conducted a vehicle checkout to ensure all systems were operating correctly after turn-on and midway to the Moon. There are two time periods where data was not available. This was due to the lander not supplying power to MAPP, leading to MAPP running on only its battery power until MAPP entered a low power state where only battery heaters were allowed to operate to conserve power. After power from the lander was reapplied, MAPP resumed the collection and sending of data. The two periods were 26 February, 23:52 MT – 27 February, 00:42 MT and 27 February, 20:31 – 28 February, 14:18 MT. There was another period of telemetry loss due to a commanding blackout from IM. This period occurred 1 March, 14:44 – 1 March, 17:42 MT. The IM-2 Nova-C lander entered lunar orbit around 3 March, 5:30pm MT and remained in orbit until the landing attempt. During this period ambient temperatures slightly increased

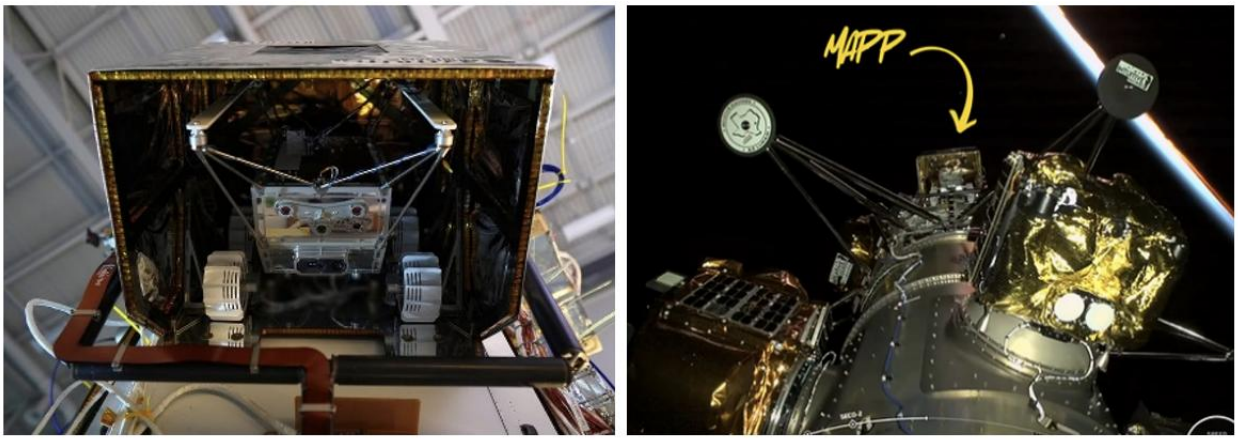


Fig. 11 | Flight Model LV1 MAPP rover during IM-2 mission. In lander deployment garage after integration onto the lander (left) and shortly after launch (right).



Fig. 12 | Mission Control rooms during IM-2 mission for Kinect operation. Lunar Outpost Mission Control operating the MAPP rover (left) and instruments during the IM-2 mission (middle), and MIT Mission Control operating the Kinect camera (right).

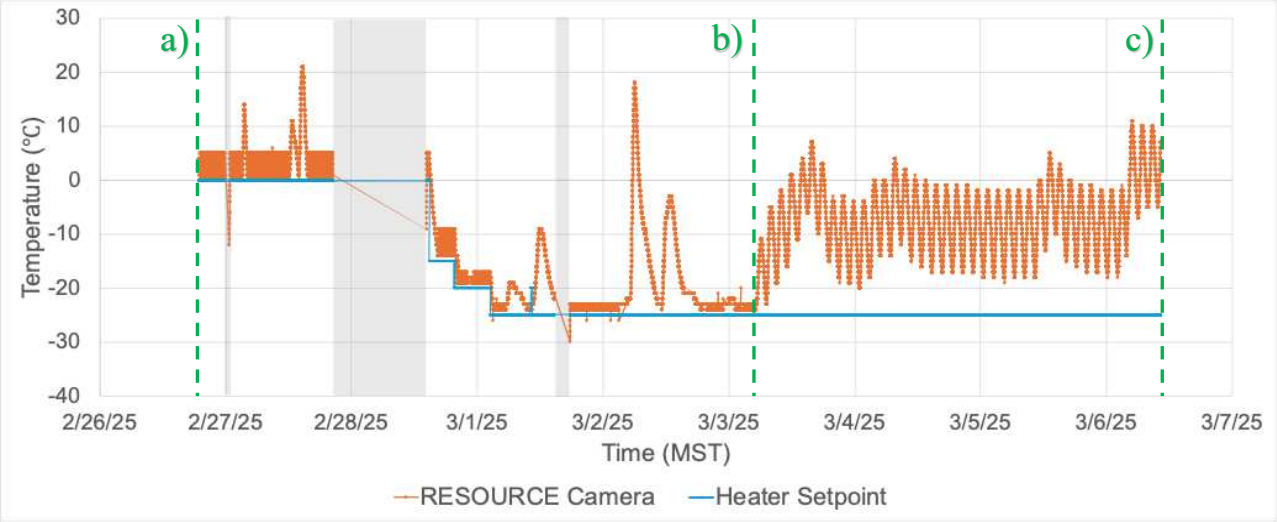


Fig. 13 | Temperature data from the onboard sensor mounted on the RESOURCE camera (thermocouple applied to top flexible surface connecting camera to MAPP body). Orange line represents the temperature of the RESOURCE camera; blue line is the heater setpoint. Dashed green lines represent significant mission events: a) launch vehicle separation and MAPP rover turn on, b) entering lunar orbit and c) landing attempt. Grey regions represent periods of telemetry loss. Data provided by Lunar Outpost.

as proximity to the Moon increased. Clear oscillations in MAPP temperature data show the cyclical nature of each orbit around the dark and lighted sides of the Moon. The IM-2 Nova-C lander attempted to land at approximately March 6, 10:32 MT, and came to rest on its side in a shaded crater. Due to the orientation of the lander in the crater, MAPP's garage was wedged upside down under the lander, preventing MAPP's deployment to the lunar surface. MAPP survived the landing and continued to run on its own battery and collect and transfer the data to the lander for the next 2.7 hours. After which it entered a power conservation mode and remains on the lunar surface.

On March 6, 2025, 20:06 MT Lunar Outpost was given permission to download data from MAPP. While in a critical low power state, the RESOURCE team were still able to successfully send a command through Lunar Outpost Stargate up to the lander and confirmation was obtained that the command was received by the lander. Operations conducted in the respective Lunar Outpost and MIT Mission Control rooms are shown in Fig. 12. IM stated that lander power died on March 6, 23:38. Temperature data from the RESOURCE camera and critical mission points are presented in Fig. 13.

3 Discussion

Through multiple testing campaigns, we demonstrated that the Microsoft Azure Kinect is a viable payload for CLPS missions to the Moon, and we successfully developed and tested a concept of operations for the mission. In this section we describe the hardware developments including ruggedization, mass reduction, and dust interference testing. The flexible, multi-modal concept of operations is described with its relevance for the IM-2 mission and future lunar missions. We also review the software development contributions and testing, describing the optimized camera settings for each mode for data rates and power consumption. The testing done to ensure each operation mode's data can be accurately rendered for cm-scale resolution is reviewed, including changes made to the initial concepts based on testing results. Finally, we review the relevance of the work in the context of current technological capabilities and mission design. Our low-cost camera was the first technology demonstration of a ToF camera for 3D surface data collection on the Moon, setting a precedent for rapid, NASA-collaborative CLPS payload development. The low cost of the COTS camera enables use of this technology and methodology on multiple future missions, increasing the availability of high-resolution surface data, and supporting the development of virtual environments of the lunar surface for geological exploration, mission planning, crew training, and public outreach.

The NASA Ames team completed rigorous hardware flight readiness testing demonstrating the RGBD camera's TRL 6 status for vacuum and vibration[13,23] and provided a lightweight version of the payload to minimize flight costs. The camera was also tested in worst-case and mission-analog scenarios for dust interference. For the mission-representative modes demonstrated on the 2024 parabolic flight, no dust interference was recorded during the lunar parabolas and only minimal interference was observed during the microgravity parabolas, neither of which would

require mitigation devices.

The four-mode concept of operations was developed to provide self-contained mission parameters that were flexible in their deployment. Given the limited advance knowledge of the landing site, it was not possible to predict a priori which features would be available for capture, or when each capture mode could be conducted. Instead, four individual concepts of operations were constructed, each specifying image capture methodology, camera settings, and power requirements, independently deployable. Specific guidelines for the overall mission, including sun angle avoidance and image stitching protocols, were also established. With the development of the AKALL[24,25] software, power consumption and data rates were tested and camera settings optimized for each capture mode. The power and data testing identified two optimized camera settings: (1) maximize depth resolution for maximum RGB image coverage (4:3 ratio) for the single capture and circumferential capture modes, and (2) minimize both RGB and depth resolution while maintaining complete overlap to maximize the number of images for the traverse and science station modes. The Svalbard field expedition established the methodology for the traverse and science station modes, demonstrating improved data capture using a raster pattern compared to a grid pattern and indicating the need to increase capture frequency from every 3 m to every 1 m. The NASA SSERVI lunar testbed experiments established the methodology for the circumferential mode, indicating that captures every 30° rather than every 60° were required for improved resolution and image stitching, and identified an optimal sun angle of 120° (or equivalently 240°) for improved image quality. The lunar testbed experiments also provided a proof-of-concept for image stitching versus video capture, demonstrating consistent reconstruction resolution for both approaches.

There is a critical lack of high-resolution (sub-meter) surface topography data at the lunar south pole, precisely the region targeted for Artemis crewed landings beginning with Artemis IV, currently planned for late 2028. The nine candidate Artemis IV landing sites identified by NASA are all within the south polar region, yet the best available elevation data (LOLA, ~10 m radial accuracy) is insufficient to resolve the meter-to-centimeter-scale features (boulders, slopes, micro-craters, regolith texture) that will determine safe EVA traverse routes, inform sample site selection, and characterize ISRU extraction surfaces. This gap represents a direct operational risk to Artemis surface missions, and cm-scale ToF depth data of the kind demonstrated here provides a pathway to address it. Additionally, areas of particular interest for science operations and ISRU, such as PSRs, are difficult to capture using photogrammetry given the absence of direct illumination. The hardware and software development pipeline demonstrated here for a COTS ToF camera supports rapid deployment on the lunar surface, and while developed and validated on the Microsoft Azure Kinect, the pipeline is transferable to other COTS products via custom software wrappers. Because these cameras combine ToF depth data with RGB imagery, they provide complete, high-resolution (sub-cm scale) 3D images of the lunar surface even in low-light environments.

Beyond data collection, the VR pipeline developed in this work has direct applications for Artemis mission preparation. Artemis astronauts will face a uniquely challenging operational environment at the south pole: near-horizontal sunlight casting long shadows, extreme thermal gradients, and terrain never before visited by humans. High-fidelity 3D VR reconstructions built from RGBD data can serve as photorealistic training environments that are impossible to replicate on Earth, allowing crews to rehearse EVA traverse routes, practice sample collection strategies at candidate geological targets, and develop intuition for scale and distance under the low-angle solar illumination conditions they will encounter[26–29] . Such VR tools have already been demonstrated for planetary geology applications in prior work from this group[8] and are directly responsive to the Artemis requirement for processed data to support tactical surface decision-making. As the cadence of Artemis south polar landings increases (NASA currently targets one crewed surface mission per year after Artemis IV) the demand for site-specific VR training data will grow substantially, and the low-cost, CLPS-deployable approach demonstrated here is well positioned to meet it.

In addition to its role as a technology demonstration, the RGBD depth-data framework developed here enables a well-defined set of surface science investigations relevant to Artemis south polar missions. The sub-cm-scale 3D topography produced by this system supports: (1) blast zone characterization: mapping changes in reflectance and regolith structure (destruction of cm-scale layering and the development of small pits, scouring marks, grooves/ridges, and stair-step structures) as a function of distance from engine plumes[30–33] , which will be critical for identifying pristine sampling zones near an Artemis HLS landing site; (2) micro-PSR and cold trap identification: resolving the cm-to-meter-scale topographic shadows[34,35] that govern cold trap distribution at scales inaccessible to orbital datasets such as LOLA; (3) small-scale roughness quantification: providing in situ cm-scale roughness measurements that constrain micrometeoroid flux, cold trap distribution, and surface trafficability[36–38] ; (4) rock and boulder mapping: measuring size-frequency distributions of pebbles (>4 mm), cobbles (>64 mm), and boulders (>256 mm) to characterize surface processing and support Artemis Base Camp site planning; (5) regolith geomechanical properties: deriving angle-of-repose and bearing capacity from rover wheel tracks and boulder tracks[39,40] , constraining cohesion, coefficient of friction, and cohesive shear strength relevant to both rover and EVA operations (the sub-cm resolution required for wheel-track and boot-print analysis is demonstrated in Fig. 6); (6) mass wasting features: identifying

rockslides, debris flows, and boulder tracks as indicators of slope stability and regolith strength[39–41] and (7) identification of water-ice in lunar regolith[23,34,35,42,43] . These science applications, while beyond the scope of the IM-2 technology demonstration reported here, are directly enabled by the ConOps and data pipeline developed in this work and provide a clear framework for proposing this capability on future CLPS missions in the Artemis science context[23,42].

The CLPS program is the robotic vanguard of NASA's Artemis initiative, tasked with scouting lunar resources, testing ISRU technologies, and returning surface data that will directly inform the selection and planning of crewed Artemis landing sites. By providing unprecedented accessibility to the space sector including rapid development timelines, fixed-price contracts, and open data sharing, CLPS is transforming what a university-scale team can contribute to the highest-priority goals in human spaceflight. The CLPS paradigm shift means that a project can go from ideation to landing on the Moon within years rather than decades, and the cost reduction ensures that a broader range of institutions can participate. The testing and development described here provides a foundational methodology for preparing low-cost COTS hardware for CLPS missions, demonstrated by the payload's readiness for rapid deployment on future flights.

While no images were acquired with the RESOURCE camera during the IM-2 mission, the results confirm two critical outcomes. Temperature data demonstrated camera survivability to −25°C, reconfirming the thermal vacuum test case, and a successful command uplink (received and acknowledged by the camera) confirmed complete software integration into the MAPP rover system. Together these results provide high confidence in the platform's functionality for future missions. Lessons learned from the IM-2 mission will be incorporated into the operations structure, and the Earth–Moon transit temperature data will inform thermal design requirements for successor payloads; a second camera could be ready for deployment in less than a year. With Artemis IV targeting a crewed south polar landing in late 2028, there remains a realistic window for one or more additional CLPS missions to deploy this system, acquire high-resolution depth data at candidate EVA sites, and deliver the VR training datasets that Artemis astronauts will require. The low development cost and demonstrated readiness of this platform make it uniquely suited to that preparatory role.

4 Methods

4.1 Hardware Selection and Flight Readiness Modifications

We explored four different types of depth-data collection techniques: 1) multi-camera stereophotogrammetry, 2) dual-lens 360° RGB imagery, 3) RGB in combination with short-range ToF and 4) long-range ToF. Using these four different techniques, we used the Boston Dynamics Spot robot to collect depth-data in a lunar analogue terrain (Marblehead, MA) including at geologically significant points of interest (POIs). We compared the techniques using five parameters: depth-of-view, field-of-view, lighting condition capabilities, resolution, and bandwidth requirements. Each technique was tested for assessment capability of the POI. With this we provided a recommendation to use an integrated RGB camera with a short-range ToF camera, resulting in what is known as an RGBD camera, for deployment on future lunar surface missions[14]. Our field tests indicated such a camera would effectively enable 3D mapping in a VR environment that is supportive of near real-time science-driven operations. 'A COTS RGBD camera was selected on the basis of commercial availability and hardware development support, then adapted for spaceflight by the NASA Ames team[13]. This initial field assessment was reported in Forsey-Smerek et al., 2022[14] and Paige et al., 2021[29].

4.1.1 RGBD camera – the Microsoft Azure Kinect

The Microsoft Azure Kinect is a ToF depth-camera with integrated RGB imagery. The camera uses modulated near-IR (NIR) light to process and generate a depth-map of a scene. The depth map is created by measuring the time it takes for the NIR light projected by the camera to return to the camera sensor based on the phase shift of the returning light. The intensity of NIR light returned from the scene is also recorded and used to create a complementary IR image. The ToF camera has different modes (narrow field of view (NFOV), wide field of view (WFOV), binned and unbinned) to allow for customization of the X- Y- and Z-axis range. The ToF camera has a pixel resolution range of 320x288 to 1024x1024 pixels and a Z-range of 0.5-5.5 m. The 12-MP RGB camera provides aspect ratios of 16:9 and 4:3. To have the RGB image completely overlap with the depth map the 4:3 aspect ratio is used with the NFOV depth setting.

4.1.2 Mission Planning

Routine operations for instrument command will be performed in line with the Lunar Outpost scheduling process. In general, the capture operations are entirely separate from the data crosslink and downlink processes to comply with the requirements from both the rover and lander. The scheduling is expected to give highest priority to the primary

rover payload, with the Kinect payload gaining higher priority later in the mission, potentially toward lunar sunset. Scheduled scenarios are not yet developed; these ConOps are flexible enough to remain fully operational throughout a variety of lighting and timing conditions.

4.2 Operational Testing Methodology

A series of tests (both lab and field) were conducted to assess the RGBD camera capabilities for lunar conditions and optimal ConOps design. We tested the power and data rates for the four capture modes, optimizing each for RGB resolution and depth resolution capture sequences. We tested the 3D reconstruction techniques and resolution capabilities in the Solar System Exploration Research Virtual Institute (SSERVI) lunar testbeds (simulated light, regolith and features) at the NASA Ames Research Center . We then used a field test in Svalbard, Norway, to design capture methodology for optimal 3D reconstruction of the traverse and Science Station capture modes. Finally, we tested the camera's capabilities with dust interference.

4.2.1 Power and Data Rates

Two of the critical limiting factors on the CLPS mission are power and data rates. As power and data rate limitations are proprietary, values will be described here as within the set limits or as exceeding these limits. The rover can only supply limited power during the operation of its multiple payloads. Additionally, while there is sufficient memory storage available on the rover for video captures, the data must be transmitted back to the lander and then back to Earth. Data download limits are set within the GB range. Given a single 10s RGBD video can require 1 GB of data, this severely limits the data collection for the RGBD camera. When starting a video recording on the Microsoft Azure Kinect, a minimum of 5 s is required to allow the image to stabilize. Some of the ConOps require views from a minimum of 12 directions, thus, this would require 120 s of video, or 120 GB of data for a single scene. However, much of the data in that 10 s video would be extraneous. The AKALL software functions by recording an initial 10 s video, then parsing a single still RGBD image from the end of the recording and saving only this image for transmission to the lander. This ensures that the image has stabilized, but that no extraneous data is being transmitted. Some data is lost using this method as gaps caused by dust, light reflection and noise can often be filled in when using multiple frames, but the data reduction allows for increased image capture albeit at a slightly lower quality.

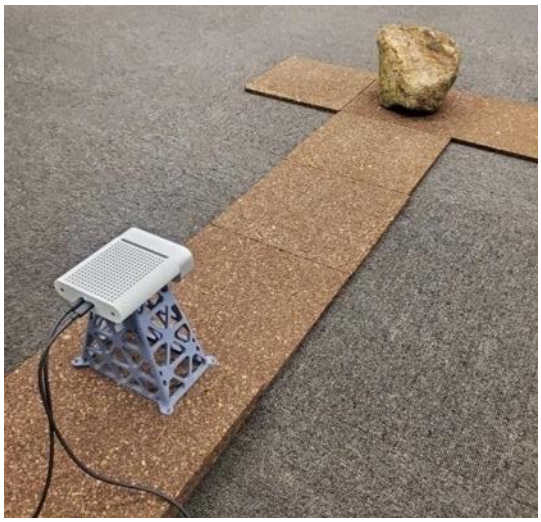


Fig. 14 | Testing configuration of the Microsoft Azure Kinect for power and data rate testing in Lunar Outpost MAPP rover configuration.

Initial power tests were done to assess the average power requirements for the different camera modes: off, idle, streaming using the SDK viewer and recording using the SDK viewer. These baseline power requirements were used to ensure the camera would a) not draw power when off, b) not draw power when idle and c) be within the mission's maximum power requirements prior to further development.

The power and data requirements for each of the capture modes were then tested in-lab by mounting an unaltered Microsoft Azure Kinect onto a custom payload tower at the height of the Lunar Outpost rover mounted Kinect (17.1 cm above the ground). Capture sequences were completed for each mode while monitoring the power. Using the AKALL software, we tested the power and data loads for different combinations of RGB resolution and ToF camera resolution. These combinations were optimized for the capture modes as follows:

1. Single capture: maximize IR/depth resolution, optimize color resolution.
2. Traverse capture: maximize number of images, minimize IR/depth resolution and color resolution.
3. Science Station capture: maximize number of images, minimize IR/depth resolution and color resolution.
4. Circumferential capture: maximize IR/depth resolution, optimize color resolution.

The experimental setup is shown in Fig. 14.

4.2.2 Lunar Analog Concept of Operations Testing: NASA SSERVI Lunar Regolith Testbed

Five testing scenarios were conducted in the NASA regolith testbed. These are listed in Table 4 along with

the metrics of study, and capture mode being assessed. For each scenario, four camera settings were used (Table 5). For tests 1 and 2, the camera was manually moved around the object at 60º intervals, maintaining a 1m distance from the object. For tests 3-5, the camera was positioned on the edge of the crater and manually adjusted for five different camera angles (yaw left and right (+/- 30º), pitch up and down (+12º/-13º), and neutral central) to demonstrate individual image capture for a potential future mission with gimballing capabilities. These were repeated for six simulated sun positions - 0º, 60º, 120º, 180º, 240º and 300º as measured from the central line of the camera with 0º behind the camera.

Table 4 | SSERVI lunar testbed JSC-1A testing scenarios with associated capture modes and metrics being tested.

Test	Capture Mode	Metrics
1 - Little rock (<10 cm)	Circumferential and Single Capture	Degrees of overlap required Resolution of rock features
2 - Big rock (>10 cm)	Circumferential and Single Capture	Degrees of overlap required Resolution of rock features
3 - Debris flow	Gimballed and Single Capture	Resolution of features (texture and depth) Gimballed image stitching vs. single video capture
4 - Crater	Gimballed and Single Capture	Gimballed image stitching vs. single video capture Optimal lighting direction
5 - Boot print	Gimballed and Single Capture	Resolution of structured feature Gimballed image stitching vs. single video capture

Table 5 | Software specifications used for the SSERVI lunar testbed experiments including resolution description, camera settings, and command sequences.

Software	Resolution	Camera settings	Control sequence
AKALL	Lunar Outpost mission	30 fps MJPG compression 2048x1536 RGB (4:3 aspect ratio) 640x576 depth (75ºx65º FOV, 0.5-3.86 m operating range) 12.8 ms exposure	K30MJPG15362
AKALL	High resolution RGB	30 fps MJPG compression 4096x3072 RGB (4:3 aspect ratio) 640x576 depth (75ºx65º FOV, 0.5-3.86 m operating range) 12.8 ms exposure	K30MJPG30722
AKALL	High resolution RGB and depth	30 fps MJPG compression 4096x3072 RGB (4:3 aspect ratio) 1024x1024 depth (120ºx120º FOV, 0.25-2.21 m operating range) 20.3 ms exposure	K30MJPG30724
Open3D	Video	30 fps MJPG compression 1280x720 RGB (16:9 aspect ratio) 512x512 depth (2x2 binned, 120ºx120º FOV, 0.25-2.88m operating range) 12.8 ms exposure	NA

4.2.3 Hardware Concept of Operations Testing: Svalbard, Norway

The Microsoft Azure Kinect was field-tested in Svalbard, Norway to assess two different capture styles, a grid-style data capture, as well as a raster-style data capture, Fig. 7.

The raster pattern provided long swathes of data side-by-side, while the grid pattern provided 360° blocks of data with central blind spots that can be partially eliminated by overlapping data from adjacent grids.

Because we could not predict the conditions of the ground on which we would be recording, we chose the simplest method to ensure camera stability: manual data collection. The camera was held at an approximately continuous height from the ground and walked in the selected pattern over the field site. This allowed for faster data collection (critical in the low temperatures) and a smoother video recording. Data was collected as .ply video recordings for complete 10m x 10m Science Station captures of three distinct field sites. A laptop computer was used to both power the Azure Kinect and record the data. Field site locations were selected based on geologically relevant water-indicating features for a virtual reality user testing experiment that was conducted in parallel to the Kinect field testing campaign for the lunar mission. Details on this study can be found in Paige et al., 2024[8]. The data captures for the lunar test campaign were used to assess ConOps for the traverse capture mode and the Science Station capture mode.

4.2.4 Dust Interference in Lunar Gravity

During the 2024 parabolic flight, data was recorded for 1 Martian gravity parabola, 3 lunar gravity parabolas and 6 microgravity parabolas. Each parabola provides approximately 20 seconds of reduced gravity followed by a period of hyper-gravity. When in reduced gravity the dust was agitated using a motorized rover wheel, simulating rover movement, and recorded the output of the RGBD camera. This gave an indication of the camera's ability to function with interfering particles and allowed monitoring of how soon after rover movement depth-data could be captured (time required for the dust to settle after agitation). After the experiment the lens of the COTS part was assessed to identify if there would be a need for a mechanism to periodically clean the lens, or if scratches would become an issue, if there would be a need for a sapphire lens, as is used on the Mars cameras[44]. The tests included assessing visibility of cm-scale representative 3D printed geological samples through dust kick-up from the rover wheel and assessing static adhesion of the lunar dust to the camera lens and any damage the dust caused.

The first experiments were run during a Zero-Gravity Corporation parabolic flight campaign on May 20, 2022, first published in Moreno et al., 2022[22] and the second was conducted on May 14th, 2024. Experimental design and results for both are summarized here. The experimental setup is shown in Fig. 10. The entire experiment was contained inside a 33 cm x 61 cm x 94 cm sealed glove box made of an 80-20 frame and polycarbonate walls. This box was covered with a dark cloth to control the sources of light. Within the box, the base was covered with approximately 2.5 cm of Lunar Highlands (LHS-1) high-fidelity Moon regolith simulant produced by the Exolith Lab[45]. The RGBD camera was mounted in the sealed glove box. The camera was recording only during the reduced gravity portion of the experiment parabolas, focused on the 3D printed rock wall mounted to the opposite side of the glove box. The rover wheel was mounted at a distance from the camera representative of the Lunar Outpost rover. The wheel was activated to disturb the lunar simulant within the glovebox and the recording was used to assess visibility loss with lunar regolith in the camera's view path.

Given this experiment was part of a shared parabolic flight campaign, the number of lunar analogous parabolas offered for that flight were limited; however, the microgravity portion of the flight served as a worst-case scenario in which all disturbed dust remained suspended. The 2022 flight used worst-case rover conditions, meaning rotating at the CLPS representative RPM (6-10 cm/s) for maximum slip and dust kick-up.

In the 2022 experiment the motor for the rover wheel and an LED light strip, used to illuminate the interior of the glovebox, were controlled by a custom printed circuit board (PCB) that was mounted to the exterior of the glove box and controlled by an Arduino Uno. The LED light was turned on as soon as the Arduino was powered. The motor had 5 different speeds that spanned from 50-300 RPM in 50 RPM increments. After every parabola, the Arduino would increase the RPM by 50. The motor was controlled by a keypad that was attached to the side of the box. The RGBD camera was connected directly to a laptop which acted as its power source and controls. For the 2024 flight the motor for the wheel was exchanged for a 5-6 RPM, 100V AC motor. The wheel was re-printed using a modified design that more closely replicated the Lunar Outpost MAPP rover design with an 18.3 cm outer diameter including traction fins. The rotation speed of the motor and the diameter of the wheel replicated the 3 m/minute speed anticipated by the MAPP rover. Given this setup maintained a consistent speed, the operation was simplified with only an on/off switch outside of the box for both motor and LED strip.

The RGBD camera was operated using the recording software provided by the Microsoft Azure Kinect Software Developer Kit (SDK). Specifically, the k4arecorder.exe operation was used. Thirty seconds of data were recorded for each parabola, saving each parabola recording to a separate file. This was done instead of continuous recording to avoid data loss mid-flight. After each parabola, a 3D printed rake, Velcro-ed to the inside wall of the box, was used to ensure no buildup of simulant was occurring behind the wheel.

Acknowledgements
Funding for the RESOURCE project was provided by SSERVI and the MIT Space Exploration Initiative. Access to the SSERVI Lunar Regolith Testbeds was provided by NASA Ames Research Center and SSERVI. The Space Exploration Initiative from the MIT Media Lab provided the opportunity to put a payload on a lunar mission and organized, funded, and ran the Svalbard expedition. Maggie Coblentz, the Svalbard expedition leader and field guide, Sean Auffinger, Svalbard and lunar mission integrator, are acknowledged for their hard work and dedication.

Competing Interests
All authors declare no financial or non-financial competing interests.

AI Disclosure
An AI agent (Claude Sonnet 4.6) was used for final review to assess final formatting, content continuity and spelling/grammatical edits. No AI agents were used for data collection, processing or analysis.

Data Availability Statement
Recorded data for all experiments are available upon request in a Dropbox repository, c.paige@columbia.edu.
Code Availability Statement: AKALL code is available on GitHub (https://github.com/sei-ml/AKALL).
Competing Interests Statement: The authors declare no competing interests.

Author Contributions:

- C. Paige – Wrote the main manuscript text. Prepared figures 4-10 and figure 14. MIT lead of the Azure Kinect camera development, ConOps development and testing (Svalbard and SSERVI Lunar regolith Lab), parabolic flight experiment lead, power and data rates co-lead. Data processing and analysis.
- D. D. Haddad – AKALL developer, data processing, software integration lead for Lunar mission. Data visualization and processing pipeline. Power and data rates co-lead.
- A. Cook – NASA Ames hardware lead. Ruggedization lead, testing and integration of hardware. Lunar mission Science team.
- V. Jha – Ruggedization, SSERVI Lunar regolith lab testing.
- A. Deutsch – Ruggedization, SSERVI Lunar regolith lab testing, Lunar mission Science team.
- J. Shimada – Ruggedization, SSERVI Lunar regolith lab testing.
- A. Colaprete – Ruggedization, testing and integration of hardware. Lunar mission Science team.
- F. Ward – ConOps development, testing at SSERVI Lunar regolith lab.
- K. Pfrang – Lunar Outpost data analysis. Prepared figures 1-3 and figures 11-13. Wrote section 2.8.
- F. Meyen – Lunar Outpost mission lead.
- A. Ekblaw – MIT To the Moon to Stay Mission PI.
- J. Heldmann – NASA RESOURCE PI.
- D. Newman – MIT RESOURCE PI.

All authors reviewed the manuscript.

References

1 NASA. Artemis III Science Definition Team Report. 2020.
2 Goecks VG, Chamitoff GE, Borissov S, Probe A, McHenry NG, Cluck N *et al.* Virtual Reality for Enhanced 3D Astronaut Situational Awareness During Robotic Operations in Space. In: *AIAA Information Systems-AIAA Infotech @ Aerospace*. American Institute of Aeronautics and Astronautics: Reston, Virginia, 2017 doi:10.2514/6.2017-0883.
3 Evelyn Miralles. An Onboard ISS Virtual Reality Trainer. In: *AIAA Modeling and Simulation Technologies*. Boston, 2013, p 20130008966.
4 Miles HC, Jones A. Designing a Virtual Toolkit for Analysing Planetary Science Data in Virtual Reality. *IEEE Trans Vis Comput Graph* 2025; **31**: 4283–4296.
5 Caravaca G, Le Mouilic S, Mangold N, L'Haridon J, Le Deit L, Masse M. 3D Digital Outcrop Model Reconstruction of the Kimberley Outcrop (Gale Crater, Mars) and It's Integration Into Virtual Reality for Simulated Geological Analysis. *Planet Space Sci* 2019; **182**. doi:https://doi.org/10.1016/j.pss.2019.104808.
6 Acevedo P, Magana AJ, Benes B, Mousas C. A Systematic Review of Immersive Virtual Reality in STEM

Education: Advantages and Disadvantages on Learning and User Experience. *IEEE Access* 2024; **12**: 189359–189386.
7 Scott DR, Malenkov MI, Head JW, Basilevsky AT. Robotic and Manned Lunar Rovers of the XX Century: The View From the XXI Century. In: *50th Lunar and Planetary Science Conference*. 2019, p 2827.
8 Paige C, Haddad DD, Piercy T, Todd J, Ward F, Ekblaw A *et al.* Development and user study of the Operational Geology in a Virtual Environment (OGIVE) platform. *Acta Astronaut* 2024; **224**: 17–36.
9 Zhao J, Wallgrün JO, LaFemina PC, Normandeau J, Klippel A. Harnessing the power of immersive virtual reality - visualization and analysis of 3D earth science data sets. *Geo-spatial Information Science* 2019; **22**: 237–250.
10 National Academies of Sciences Engineering and Medicine. *Origins, Worlds, and Life: a decadal strategy for planetary science and astrobiology 2023-2032*. National Academies Press: Washington, D.C., 2022 doi:10.17226/26522.
11 NASA. Artemis Plan: NASA's Lunar Exploration Program Overview. 2020.
12 Caravaca G, Le Mouilic S, Mangold N, L'Haridon J, Le Deit L, Masse M. 3D Digital Outcrop Model Reconstruction of the Kimberley Outcrop (Gale Crater, Mars) and It's Integration Into Virtual Reality for Simulated Geological Analysis. *Planet Space Sci* 2019; **182**. doi:https://doi.org/10.1016/j.pss.2019.104808.
13 Plan A. NASA's Lunar Exploration Program Overview. 2020.
14 Jha V, Garrett M, White B, Shimada J, Cook A, Colaprete A *et al.* Ruggedizing a Commercial Depth Camera for Novel Lunar Exploration. In: *AGU Fall Meeting Abstracts*. 2022, pp P55E-1617.
15 Forsey-Smerek F, Paige C, Ward F, Haddad DD, Sanneman L, Todd J *et al.* Assessment of Depth Acquisition Methods for Virtual Reality Mission Operations Support Tools. In: *IEEE Aerospace Conference Proceedings*. 2022.
16 Haddad DD, Paige C, Ward F, Paradiso JA, Newman D, Ekblaw A *et al.* Azure Kinect à La Luna (AKALL): Leveraging Low-Cost RGB and Depth-Camera in Lunar Exploration. In: *2024 IEEE Aerospace Conference*. IEEE, 2024, pp 1–9.
17 Park J, Zhou QY, Koltun V. Colored point cloud registration revisited. In: *IEEE Conference on Computer Vision and Pattern Recognition*. 2017, pp 143–152.
18 Choi S, Zhou QY, Koltun V. Robust reconstruction of indoor scenes. In: *IEEE Conference on Computer Vision and Pattern Recognition*. 2015, pp 5556–5565.
19 Zhou Q-Y, Park J, Koltun V. Open3D: A modern library for 3D data processing. *arXiv preprint* 2018.
20 Paige CA, Haddad DD, Ward F, Todd J, Osinski G, Ekblaw A *et al.* Data collection in Svalbard, Norway to test the use of virtual reality for Lunar and planetary surface exploration. In: *International Conference on Environmental Systems*. 2023, p 362.
21 Garland M, Heckbert PS. Surface simplification using quadric error metrics. In: *Proceedings of the 24th annual conference on Computer graphics and interactive techniques, ACM*. 1997, pp 209–216.
22 Johansen MR. NASA Dust Mitigation Strategy. In: *The Impacts of Lunar Dust on Human Exploration*. 2020.
23 Moreno MRA, Paige CA, Stober J, Rupasinghe J, Wood D, Newman D. Capturing the Moon: 3D Mapping and Regolith Collection for Low-Cost Lunar Rover Missions. In: *ASCEND*. 2022 doi:10.2514/6.2022-4285.
24 Cook AM, Paige C, Haddad DD, Ekblaw A, Auffinger S, Heldmann J *et al.* Moon3D: A Depth-Mapping Camera for Lunar Environmental and Geophysical Studies. In: *Lunar Surface Science Workshop (LSSW) 25: Plume-Surface Interactions*. 2024, pp 3074–5007.
25 Haddad DD, Unterhauser S, Paige CA, Brokaw B, Ward F, Paradiso J *et al.* Leveraging Docker Containers for Azure Kinect Integration in Space Robotics: An Overview of the Azure Kinect a La Luna (AKALL) Framework. In: *SpaceCHI2*. 2023.
26 Haddad DD, Paige C, Ward F, Cook A, Heldmann J, Paradiso JA *et al.* Azure Kinect `a La Luna (AKALL): Leveraging Low-Cost RGB and Depth-Camera in Lunar Exploration. In: *IEEE Aerospace Conference*. 2024.
27 Paige CA, Ward F, Haddad DD, Todd J, Newman D. Assessing Virtual Reality for Remote Lunar Geological Fieldwork. In: *Lunar Surfaces Science Workshop*. 2022.
28 Paige CA, Newman D, Haddad DD, Ward F, Piercy T. Lunar instrument data integration into the Virtual Reality Mission Simulation System for Decision Making and Situational Awareness. In: *International Conference on Environmental Systems*. 2021, p 227.
29 Paige CA, Haddad DD, Piercy TJ, Todd JE, Ekblaw A, Newman D. Development and user study of the Operational Geology in a Virtual Environment (OGIVE) platform. *Acta Astronaut* 2024; **224**: 17–36.
30 Paige CA, Forsey-Smerek A, Haddad DD, Ward F, Piercy TJ, Heldmann J *et al.* A virtual reality platform

for lunar rover missions to reduce decision-making time and improve situational awareness. In: *ASCEND*. 2021.
31 Immer C, Metzger P, Hintze PE, Nick A, Horan R. Apollo 12 Lunar Module exhaust plume impingement on Lunar Surveyor III. *Icarus* 2011; **211**: 1089–1102.
32 Kaydash V, Shkuratov Y, Korokhin V, Videen G. Photometric anomalies in the Apollo landing sites as seen from the Lunar Reconnaissance Orbiter. *Icarus* 2011; **211**: 89–96.
33 Clegg-Watkins RN, Jolliff BL, Boyd A, Robinson MS, Wagner R, Stopar JD *et al.* Photometric characterization of the Chang'e-3 landing site using LROC NAC images. *Icarus* 2016; **273**: 84–95.
34 Clegg RN, Jolliff BL, Robinson MS, Hapke BW, Plescia JB. Effects of rocket exhaust on lunar soil reflectance properties. *Icarus* 2014; **227**: 176–194.
35 Haddad DD, Paige CA, Ekblaw A, Paradiso J, Newman D, Cook A *et al.* RGB-NIR Reflectance and 3D Microtopography for Lunar Regolith Analysis Using ToF Imaging Systems. In: *IEEE Aerospace Conference*. 2026.
36 Haddad DD, Deutsch AN, Colaprete A, Cook AM, Paige C, Perry E *et al.* Measuring reflectance and maturity of lunar regolith and permafrost simulants using visible-near infrared wavelengths. In: *56th Lunar and Planetary Science Conference (LPSC)*. 2025, p 2679.
37 Palmer EM, Heggy E, Patterson G. The Importance of Understanding Surface Roughness for Human Exploration of the Moon: Volatile Mapping and Assessing Surface Trafficability. In: *American Geophysical Union, Fall Meeting 2019*. 2019, pp P51D-3406.
38 Plescia JB, Cahill J, Greenhagen B, Hayne P, Mahanti P, Robinson MS *et al.* Lunar Surface Processes. *Rev Mineral Geochem* 2023; **89**: 651–690.
39 Cai Y, Fa W. Meter-Scale Topographic Roughness of the Moon: The Effect of Small Impact Craters. *J Geophys Res Planets* 2020; **125**. doi:10.1029/2020JE006429.
40 Sargeant HM, Bickel VT, Honniball CI, Martinez SN, Rogaski A, Bell SK *et al.* Using Boulder Tracks as a Tool to Understand the Bearing Capacity of Permanently Shadowed Regions of the Moon. *J Geophys Res Planets* 2020; **125**. doi:10.1029/2019JE006157.
41 Bickel VT, Kring DA. Lunar south pole boulders and boulder tracks: Implications for crew and rover traverses. *Icarus* 2020; **348**: 113850.
42 Bickel VT, Honniball CI, Martinez SN, Rogaski A, Sargeant HM, Bell SK *et al.* Analysis of Lunar Boulder Tracks: Implications for Trafficability of Pyroclastic Deposits. *J Geophys Res Planets* 2019; **124**: 1296–1314.
43 Deutsch AN, Paige CA, Ward FS, Cook AM, Jha V, Shimada J *et al.* Lunar surface science with a Microsoft Kinect depth camera: Experiments in the SSERVI regolith testbed. In: *NASA Exploration Science Forum*. 2023.
44 Paige C, Haddad DD, Fortuin C, Pearson M, Deutsch A, Cook AM *et al.* 3D ToF–RGB/NIR Imaging of Antarctic Lunar Analogs for Geotechnical and Volatile Assessment in ISRU Drilling Operations. In: *55th International Conference on Environmental Systems*. San Juan, 2026, pp 553–553.
45 Bell JF, Squyres SW, Herkenhoff KE, Maki J, Schwochert M, Dingizian A *et al.* The Panoramic Camera (PanCam) Investigation on the NASA 2003 Mars Exploration Rover Mission. In: *Lunar and Planetary Science XXXIV*. 2003, p 1980.
46 Long-Fox JM, Britt DT. Characterization of planetary regolith simulants for the research and development of space resource technologies. *Frontiers in Space Technologies* 2023; **4**. doi:10.3389/frspt.2023.1255535.